Hemodynamic analysis of bladder tumors using T 1-dynamic contrast-enhanced fast spin-echo MRI

doi: 10.1016/j.ejrad.2011.04.013

Hemodynamic analysis of bladder tumors using T_1-dynamic contrast-enhanced fast spin-echo MRI

ABSTRACT

Objectives: To evaluate the hemodynamics of bladder tumors, we developed a method to calculate change in R_1 value (ΔR_1) from T_1-dynamic contrast-enhanced fast spin-echo magnetic resonance imaging (T_1DCE-FSE-MRI).

Materials and Methods: On a 1.5-T MR system, T_1DCE-FSE-MRI was performed. This study was applied to 12 patients with urinary bladder tumor, i.e. urothelial carcinoma. We compared ΔR_1- and ΔSI-time between a peak in the ΔR_1- and ΔSI-time curve occurred during the first pass within 60 s. Next, we assessed the slope of increase for 180 s after CA injection ($Slope_{0\text{-}180}$).

Results: The mean slope of the first pass was significantly higher for bladder tumors on both the ΔR_1- and the ΔSI- time curve compared with normal bladder walls. Moreover, a significant difference was apparent between bladder tumors and normal bladder walls on the mean $Slope_{0\text{-}180}$ in the ΔR_1-time curve. However, no significant difference in the mean $Slope_{0\text{-}180}$ was observed on the ΔSI-time curve between bladder tumors and normal bladder walls.

Conclusion: T_1DCE-FSE-MRI offers three advantages: quantitative analysis; high-quality (i.e., artifact-free) images; and high temporal resolution even for SE

images. Use of ΔR_1 analysis with T_1DCE-FSE-MRI allows more detailed information on the hemodynamics of bladder tumors to be obtained and assists in differentiation between bladder tumors and the normal bladder wall.

Key Words: dynamic contrast-enhanced MRI (DCE-MRI); bladder tumors; hemodynamics; relaxation rate; fast spin-echo

INTRODUCTION

Cystoscopy has initially been used for the diagnosis of bladder tumors, and biopsy has generally been performed for the localized diagnosis and characterization of tumors. Treatment and prognosis are primarily determined by the invasion depth of tumors and the extent of metastases (i.e., staging) [1]. Magnetic resonance imaging (MRI) is used for staging of bladder tumors, with invasion depth the key characteristic used to define disease stage [2, 3]. To assess the staging of bladder tumors, T_2-weighted imaging [2], diffusion-weighted (DW) imaging [4], and dynamic contrast-enhanced MRI (DCE-MRI) have been used [4-8]. In particular, DCE-MRI enables successful separation of bladder tumors from muscle in the early phase. Narumi et al [6] demonstrated that oblique DCE-MRI with the spin-echo (SE) method showed high staging accuracy, particularly in differentiating between superficial tumors and tumors with superficial muscle invasion. Barentsz et al [7] also reported that evaluation of chemotherapy in advanced bladder tumors could be performed using DCE-MRI, it helped detect 13 of 14 responders and eight of eight nonresponders after two chemotherapy cycles.

In DCE-MRI techniques in oncology, acquisition of serial T_1-weighted images is

widely used, and hemodynamics of the tumor are assessed using the signal intensity (SI) or change in SI (ΔSI). However, the relationship between the SI and the concentration of contrast agent (CA) is not linear [9]. To assess the exact hemodynamics of the tumor characterization by means of pharmacokinetics analysis, inversed T_1 (R_1) values that are linearly proportional to the concentration of CA must be calculated [10].

We therefore developed a method to calculate change in R_1 value (ΔR_1) from the dynamic contrast-enhanced fast spin-echo (FSE) sequence, and used this method to evaluate the hemodynamics of bladder tumors. We describe the basis of this method and its clinical usefulness below.

MATERIALS AND METHODS

Imaging Procedure and Imaging Analysis

On a 1.5-T MRI system (Intera Achieva 1.5-T; Philips Medical Systems, Best, The Netherlands), patients were placed in a supine position with a 5-element phased-array coil (as a receiver) wrapped around the pelvis. To achieve moderate bladder distension, all patients drank 200 mL of water 30 min before MRI.

To calculate the T_1 value of pre-contrast tissue (T_{10}), FSE with spectral presaturation with inversion recovery (SPIR) sequences were performed with two repetition times (TR: $2TR_1=TR_2$, i.e., TR_1=600 ms and TR_2=1200 ms). The other imaging parameters were 6 ms echo time, 9 echo train length, 192 x 256 matrix, 300 mm field of view, 15 slices, 4 mm slice thickness, and 0.4 mm intersection gap. In addition, pre-saturation slabs parallel to the slices were applied to suppress inflow effects. Data acquisition was combined using a parallel imaging technique and a phase oversampling technique to suppress aliasing artifacts.

Then, gadolinium-diethylenetriamine pentaacetic acid (Gd-DTPA BMA; Omniscan, Daiichi-Sankyo, Tokyo, Japan) at a dose of 0.1 mmol/kg of body weight was administered intravenously using an MR-compatible power injector (Sonic Shot 50, Nemoto, Tokyo, Japan) at a rate of 2.0 mL/s, followed by bolus injection of 15 mL saline flash. Concurrently, a series of 150 images at 10 time points using FSE with SPIR, that is, identical to the pre-contrast sequence 600 ms TR, was acquired with a temporal resolution of 20 s. The other imaging parameters were set identically at pre-contrast.

We measured SIs (pre-contrast SI: I_{1pre}, I_{2pre}; post-contrast SI: I_{post}) by drawing

regions of interest (ROI) on the tumor and normal bladder wall in each patient. We then set the ROI size for a minimum of 10 pixels. T_{10} and post-contrast T_1 (T_{1post}) were calculated using the follow equations [11].

$$T_{10} = -TR_1 / \ln\{(I_{2pre} - I_{1pre}) / I_{1pre}\} \quad [1]$$

$$T_{1post} = -TR_{post} / \ln[(-I_{post} / I_{pre}) \bullet \{1 - \exp(-TR_{post} / T_{10})\} + 1] \quad [2]$$

where TR_{post} is post-contrast TR. Moreover, we calculated ΔR_1 using the following equation:

$$\Delta R_1 = 1/T_{1post} - 1/T_{10} \quad [3]$$

Then, we compared ΔR_1- and ΔSI-time between a peak in the ΔR_1- and ΔSI-time curve occurred during the first pass within 60 s. Next, we assessed the slope of increase for 180 s after CA injection ($Slope_{0\text{-}180}$).

Study Subjects

We examined 12 patients (nine men, three women; mean age ± standard deviation, 74.5 ± 7 years; range, 61-87 years) with bladder tumors. Table 1 shows patient characteristics. Pathological diagnosis was urothelial carcinoma (i.e., transitional cell carcinoma) in all patients. Histopathological confirmation was obtained in all subjects by transurethral resection and cystectomy. Comparisons between ΔR_1 and

ΔSI were made using the nonparametric Wilcoxon signed rank test. Statistical analysis was performed using Prism 5 version 5.0b statistical software (GraphPad Software, San Diego, CA). $P < 0.05$ was considered statistically significant. This study was approved by the internal review board of our Hospital. Informed consent was obtained from all patients.

RESULTS

Imaging acquisitions were successfully performed for all patients. Consequently, ΔR_1 were calculated for all case. MR images of two clinical cases are shown in Fig. 1 and Fig. 2

The mean slope of the first pass was significantly higher for bladder tumors on the ΔR_1-time curve compared with normal bladder walls ($P = 0.0156$; bladder tumor, 0.090 ± 0.04 s^{-2}; normal bladder wall, 0.015 ± 0.01 s^{-2}) (Fig. 3a). The mean slope of the first pass was also significantly higher for bladder tumors on the ΔSI-time curve than for normal bladder walls ($P = 0.0223$) (Fig. 3b).

Moreover, a significant difference was apparent between bladder tumors and normal bladder walls on the mean $Slope_{0\text{-}180}$ in the ΔR_1-time curve ($P = 0.0313$;

bladder tumor, 0.017 ± 0.008 s^{-2}; normal bladder wall, 0.007 ± 0.004 s^{-2}) (Fig. 4a). However, no significant difference in the mean $Slope_{0\text{-}180}$ was observed on the ΔSI-time curve between bladder tumors and normal bladder walls (P = 0.0625) (Fig. 4b).

DISCUSSION

We developed a method to calculate ΔR_1 from the dynamic contrast-enhanced FSE sequence, and used this method to evaluate the hemodynamics of bladder tumors. Figure 5 shows an overview of findings of this study. Changes in ΔR_1- and ΔSI-time curve of the bladder tumors demonstrated two patterns: one group (n = 7) showed a peak during the first pass, and the other group (n = 5) showed a rapid increase for 180 s. The significant difference between bladder tumor and normal bladder wall groups when assessing the mean gradient of the ΔR_1-time curve exceeded that of the ΔSI-time curve assessment, indicating the utility of ΔR_1 analysis. Relationships between ΔR_1 and CA concentration are linear, which enables the acquisition of detailed and quantitative hemodynamic information on bladder tumors.

Some reports have been published showing the high accuracy of staging of bladder tumors with DCE-MRI using SE or FSE methods [4-6]. Other studies have demonstrated the ability to track responses to chemotherapy with DCE-MRI with the gradient-echo (GRE) method [7]. However, in these techniques, imaging of a slice or a few slices was acquired from within the target of bladder tumor; thus, these methods did not include the whole bladder. Bladder tumors, in general, have a high risk of multiple and/or recurrence [12]. We could obtain satisfactory slices, that is, all bladder images within a thin slice, by using this optimized technique and a temporal resolution of 20 s. Besides, we could obtain high-quality images as conventional clinical SE images in using this method. Therefore, this method may be more useful for assisting in the diagnosis of bladder tumors and for assessing response to therapy, such as chemo-radiotherapy or arterial injection of chemotherapy.

In general, the pulse sequence for DCE-MRI is performed using a GRE sequence, that is, spoiled GRE [13, 14]. Moreover, several methods for T_1 quantification have been described. Particularly, the two-flip-angle spoiled GRE method for the calculation of T_1 is the possibility of obtaining high spatial resolution and large

volume coverage in a relatively short acquisition time. However, it has been reported that various effects may render the method vulnerable to systematic errors and instabilities (e.g., radio frequency [RF] spoiling, the spatial variability of the FA, and a systematic noise bias in the case of low SNR)[15]. In the pelvic MR imaging, the GRE causes much greater susceptibility artifacts due to the effects of inhomogeneity of the magnetic field (e.g., pericystic bowel gas). The FSE sequence used in this study, which was refocused with a 180˚ pulse, leads to absence of influence of inhomogeneity of the magnetic field and thus greatly reduces the susceptibility effect [16, 17]. Therefore, the main advantage of this method is T_1 quantification with stable spin-echo signal data instead of unstable free induction decay signal data used in GRE.

On the other hand, as a limitation of this method, a high-velocity signal loss effect has been seen using the SE method [18]. For this effect, blood signals in the artery or rapid flow structure might not be fully acquired. Therefore, when the artery input function for pharmacokinetic analysis is measured using this method, we must select the best slice section or slice orientation without a high-velocity signal loss effect.

Additionally, we could obtain T_{10} values with this method. Mean values of T_{10} of the bladder tumors and normal bladder walls were 1.295 ± 0.209 s and 0.923 ± 0.242 s (P = 0.0049), respectively (Fig. 6). Thus, T_{10} may provide additional information for diagnosis [19]. However, T_{10} values do not provide enough data to make a diagnosis, as is seen with ΔR_1 analysis with hemodynamic evaluation.

CONCLUSIONS

T_1DCE-FSE-MRI offers three advantages: quantitative analysis; high-quality (i.e., artifact-free) images; and high temporal resolution even for SE images. Use of ΔR_1 analysis with T_1DCE-FSE-MRI allows more detailed information on the hemodynamics of bladder tumors to be obtained and assists in differentiation between bladder tumors and the normal bladder wall.

REFERENCES

[1] Kern WH. The grade and pathologic stage of bladder cancer. Cancer 1984;53(5):1185-9.

[2] Fisher MR, Hricak H, Tanagho EA. Urinary bladder MR imaging. Part II. Neoplasm. Radiology 1985;157(2):471-7.

[3] Buy JN, Moss AA, Guinet C, et al. MR staging of bladder carcinoma:

correlation with pathologic findings. Radiology 1988;169(3):695-700.

[4] Tachibana M, Baba S, Deguchi N, et al. Efficacy of gadolinium-diethylenetriaminepentaacetic acid-enhanced magnetic resonance imaging for differentiation between superficial and muscle-invasive tumor of the bladder: a comparative study with computerized tomography and transurethral ultrasonography. J Urol 1991;145(6):1169-73.

[5] Tanimoto A, Yuasa Y, Imai Y, et al. Bladder tumor staging: comparison of conventional and gadolinium-enhanced dynamic MR imaging and CT. Radiology 1992;185(3):741-7.

[6] Narumi Y, Kadota T, Inoue E, et al. Bladder tumors: staging with gadolinium-enhanced oblique MR imaging. Radiology 1993;187(1):145-50.

[7] Barentsz JO, Berger-Hartog O, Witjes JA, et al. Evaluation of chemotherapy in advanced urinary bladder cancer with fast dynamic contrast-enhanced MR imaging. Radiology 1998;207(3):791-7.

[8] Tekes A, Kamel I, Imam K, et al. Dynamic MRI of bladder cancer: evaluation of staging accuracy. AJR Am J Roentgenol 2005;184(1):121-7.

[9] Rosen BR, Belliveau JW, Vevea JM, Brady TJ. Perfusion imaging with

NMR contrast agents. Magn Reson Med 1990;14(2):249-65.

[10] Heiland S, Benner T, Debus J, Rempp K, Reith W, Sartor K. Simultaneous assessment of cerebral hemodynamics and contrast agent uptake in lesions with disrupted blood-brain-barrier. Magn Reson Imaging 1999;17(1):21-7.

[11] Kanazawa Y, Miyati T, Inoue Y, Sato O. [Evaluation of imaging parameters for T1 dynamic contrast enhanced MRI with fast spin-echo]. Nippon Hoshasen Gijutsu Gakkai Zasshi 2007;63(10):1127-32.

[12] Sylvester RJ, Oosterlinck W, Witjes JA. The schedule and duration of intravesical chemotherapy in patients with non-muscle-invasive bladder cancer: a systematic review of the published results of randomized clinical trials. Eur Urol 2008;53(4):709-19.

[13] Rijpkema M, Kaanders JH, Joosten FB, van der Kogel AJ, Heerschap A. Method for quantitative mapping of dynamic MRI contrast agent uptake in human tumors. J Magn Reson Imaging 2001;14(4):457-63.

[14] Choyke PL, Dwyer AJ, Knopp MV. Functional tumor imaging with dynamic contrast-enhanced magnetic resonance imaging. J Magn Reson Imaging 2003;17(5):509-20.

[15] Preibisch C, Deichmann R. Influence of RF spoiling on the stability and accuracy of T1 mapping based on spoiled FLASH with varying flip angles. Magn Reson Med 2009;61(1):125-35.

[16] Constable RT, Kennan RP, Puce A, McCarthy G, Gore JC. Functional NMR imaging using fast spin echo at 1.5 T. Magn Reson Med 1994;31(6):686-90.

[17] Reimer P, Allkemper T, Schuierer G, Peters PE. Brain imaging: reduced sensitivity of RARE-derived techniques to susceptibility effects. J Comput Assist Tomogr 1996;20(2):201-5.

[18] Bradley WG, Jr., Waluch V. Blood flow: magnetic resonance imaging. Radiology 1985;154(2):443-50.

[19] Kershaw LE, Hutchinson CE, Buckley DL. Benign prostatic hyperplasia: evaluation of T1, T2, and microvascular characteristics with T1-weighted dynamic contrast-enhanced MRI. J Magn Reson Imaging 2009;29(3):641-8.

Figure Legends

Fig. 1. A 61-year-old male with urothelial carcinoma (Patient No. 3). Transverse FSE T_2- (**a**) and T_1- (**b**) weighted images. **c**, **d**: Transverse FSE with SPIR images were performed with two repetition times (TR: $2TR_1=TR_2$, i.e., TR_1=600 ms image [**c**] and TR_2=1200 ms image [**d**]) to calculate the T_1 value of pre-contrast tissue. **e**: Transverse dynamic contrast-enhanced FSE with SPIR images of this case. A series at 10 time points using FSE, that is, identical to the pre-contrast sequence 600 ms TR, was acquired with a temporal resolution of 20 s. Images were acquired after intravenous bolus Gd-DTPA injection, from left to right and top to bottom. **f**: Time-ΔR_1 curve of this case in ROI analysis.

Fig. 2. A 80-year-old male with urothelial carcinoma (Patient No. 11). Transverse FSE T_2- (**a**) and T_1- (**b**) weighted images. **c**, **d**: Transverse FSE with SPIR images were performed with two repetition times (TR: $2TR_1=TR_2$, i.e., TR_1=600 ms image [**c**] and TR_2=1200 ms image [**d**]) to calculate the T_1 value of pre-contrast tissue. **e**: Transverse dynamic contrast-enhanced FSE with SPIR images of this case. A series at 10 time points using FSE, that is, identical to the pre-contrast sequence 600 ms TR, was acquired with a temporal resolution of 20 s.

Images were acquired after intravenous bolus Gd-DTPA injection, from left to right and top to bottom. **f**: Time-ΔR_1 curve of this case in ROI analysis.

Fig. 3. Boxplots showing relationship between bladder tumors and normal bladder wall in the first pass slope. (a) ΔR_1 analysis. (b) ΔSI analysis. The horizontal line is the median, the ends of the box are the upper and lower quartiles, and the vertical lines are the full range of values in the data, respectively.

Fig. 4. Boxplots showing the relationship between bladder tumors and normal bladder wall in the $Slope_{0\text{-}180}$. (a) ΔR_1 analysis. (b) ΔSI analysis. The horizontal line is the median, the ends of the box are the upper and lower quartiles, and the vertical lines are the full range of values in the data, respectively. NS: not significant.

Fig. 5. Overview of this study.

Fig. 6. Boxplots showing relationship between bladder tumors and normal bladder

wall in the T_{10}-derived FSE method. The horizontal line is the median, the ends of the box are the upper and lower quartiles, and the vertical lines are the full range of values in the data, respectively.

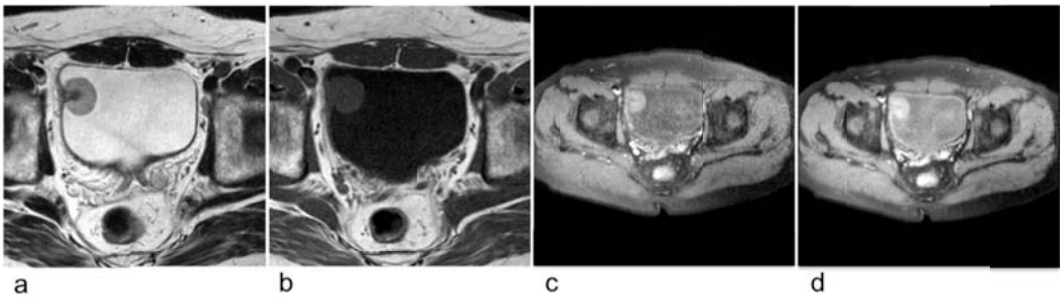
a
b
c
d

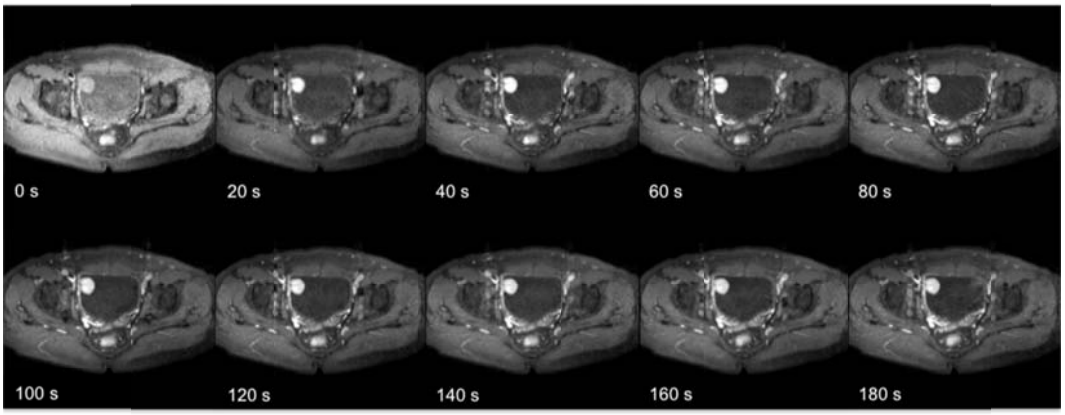
0 s
20 s
40 s
60 s
80 s
100 s
120 s
140 s
160 s
180 s
e

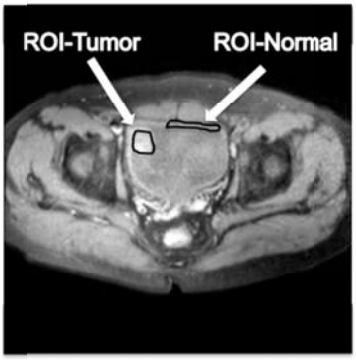
ROI-Tumor
ROI-Normal
f

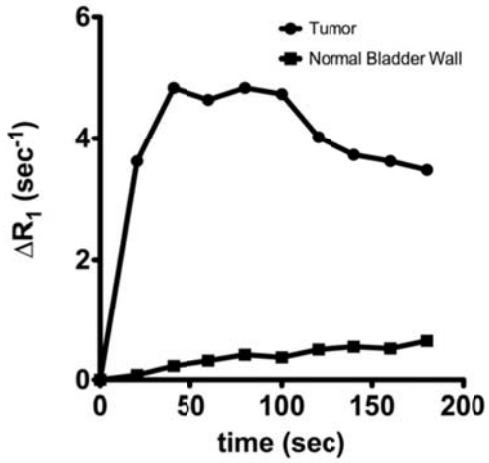
Tumor
Normal Bladder Wall
ΔR1 (sec-1)
6
4
2
0
0
50
100
150
200
time (sec)
g

Fig.1

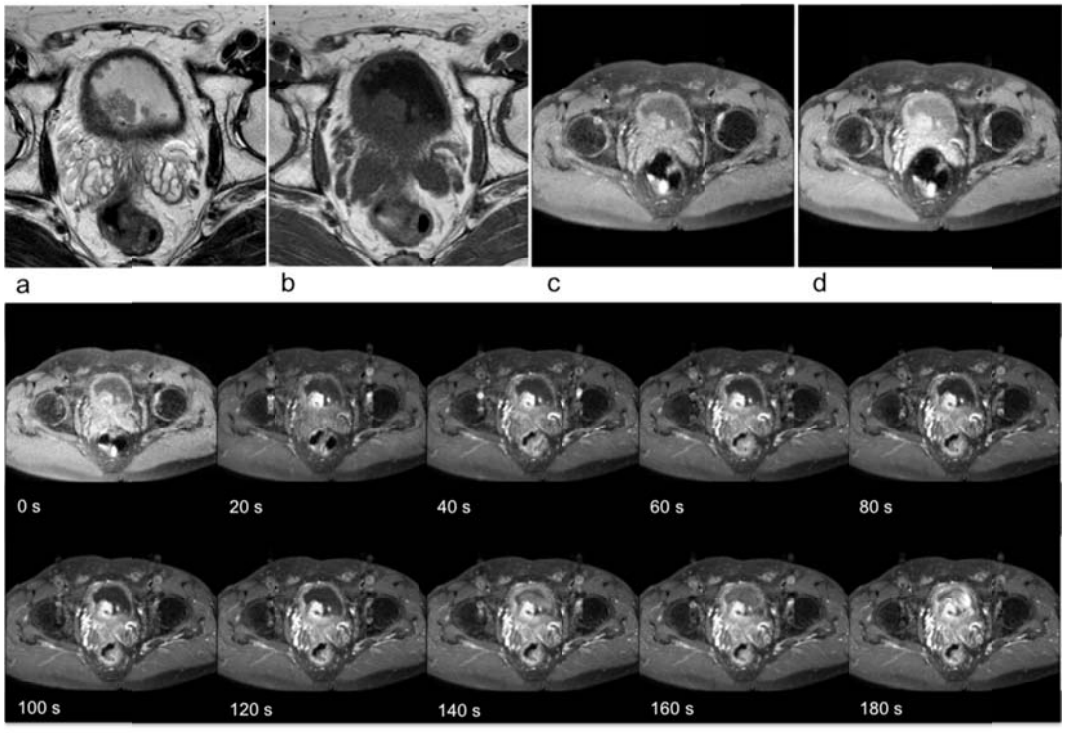
a
b
c
d
0 s
20 s
40 s
60 s
80 s
100 s
120 s
140 s
160 s
180 s
e

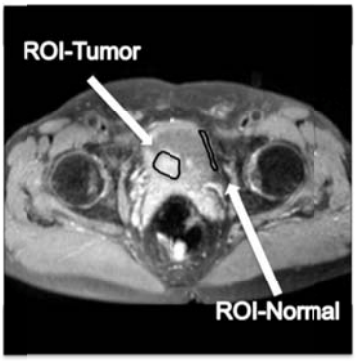
ROI-Tumor
ROI-Normal
f

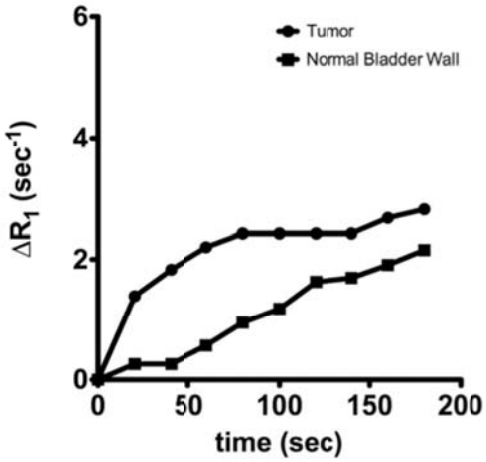
Tumor
Normal Bladder Wall
ΔR1 (sec-1)
0
2
4
6
0
50
100
150
200
time (sec)
g

Fig. 2

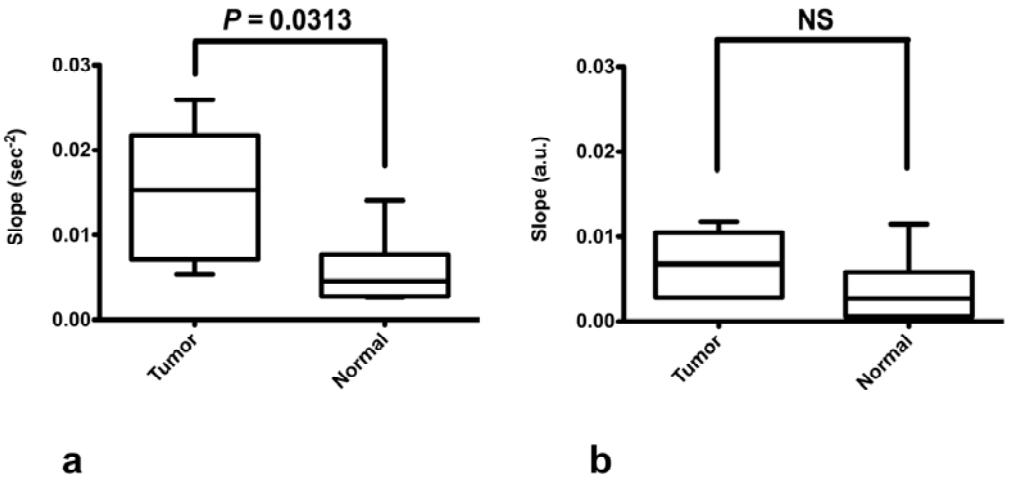
P = 0.0313
Slope (sec-2)
0.03
0.02
0.01
0.00
Tumor
Normal
a
NS
Slope (a.u.)
0.03
0.02
0.01
0.00
Tumor
Normal
b

Fig. 3

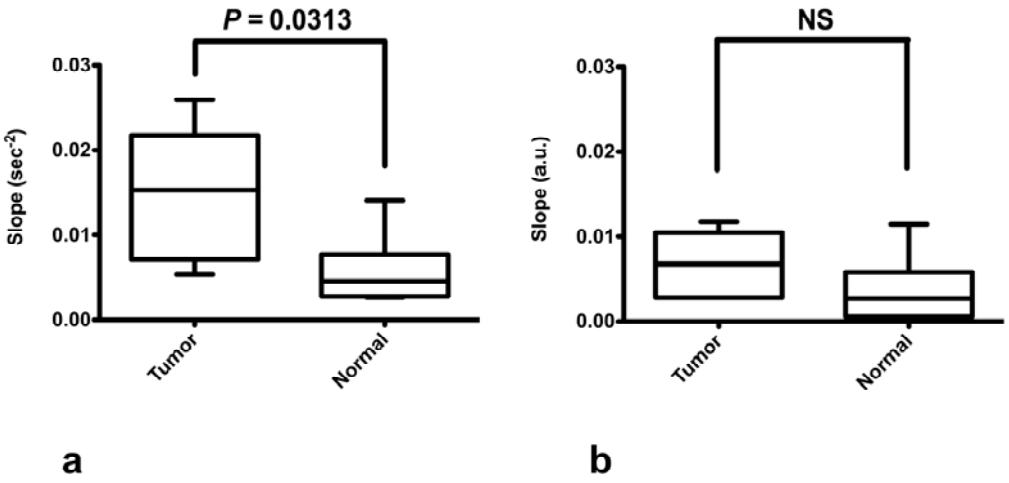
P = 0.0313
Slope (sec-2)
0.03
0.02
0.01
0.00
Tumor
Normal
a
NS
Slope (a.u.)
0.03
0.02
0.01
0.00
Tumor
Normal
b

Fig. 4

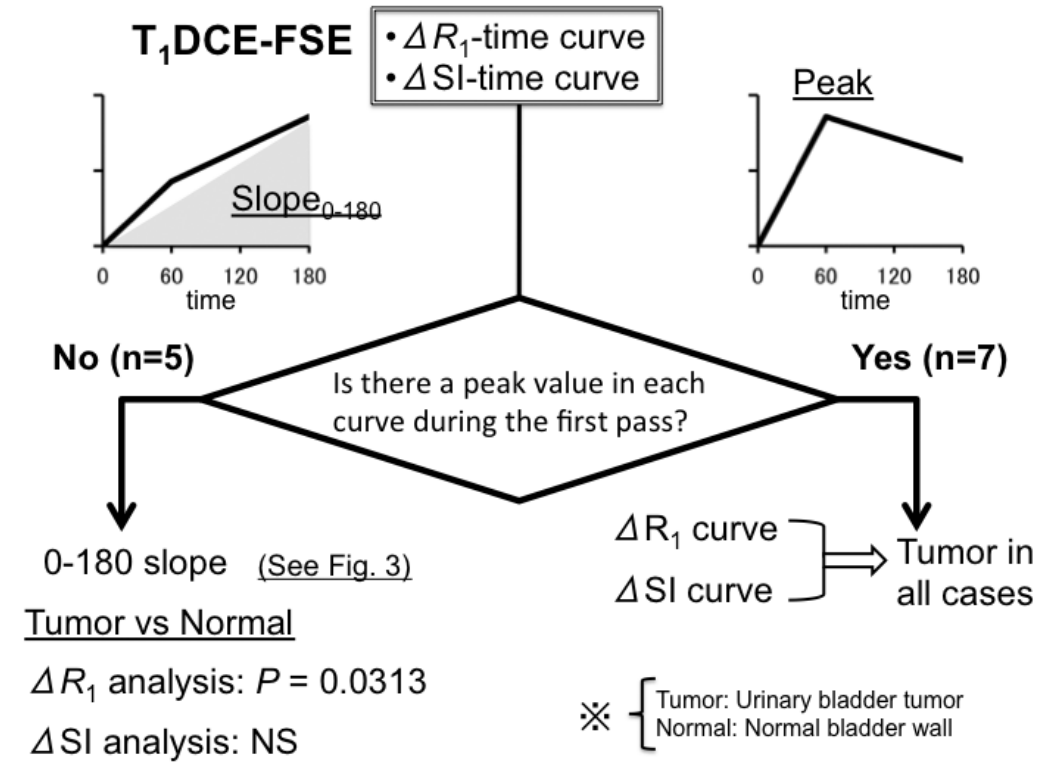
T1DCE-FSE
• ΔR1-time curve
• ΔSI-time curve
Slope0-180
0 60 120 180
time
Peak
0 60 120 180
time
No (n=5)
Is there a peak value in each curve during the first pass?
Yes (n=7)
0-180 slope (See Fig. 3)
Tumor vs Normal
ΔR1 analysis: P = 0.0313
ΔSI analysis: NS
ΔR1 curve
ΔSI curve
Tumor in all cases
※
Tumor: Urinary bladder tumor
Normal: Normal bladder wall

Fig. 5

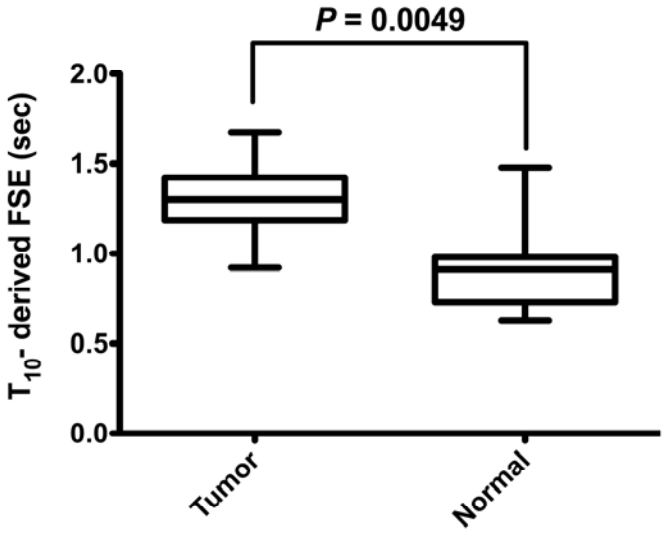

Fig. 6

Table 1 Characteristics of patients

Patient No.	Sex	Age	WHO Grade	Histopathologic Stage	Means of Histopathologic Staging
1	Male	67	G2 > G1	pT1	TUR-Bt
2	Female	72	G2	≧pT2a	TUR-Bt
3	Male	61	G3	pT2b	TUR-Bt
4	Male	70	G2	pT2b	TUR-Bt
5	Male	72	G2	pT1	TUR-Bt
6	Male	72	G2	pT2b	TUR-Bt
7	Female	75	G3	pT2a	TUR-Bt
8	Male	80	G2	pTis	TUR-Bt
9	Male	85	G2	pT1a	TUR-Bt
10	Female	87	G2	≧pT2b	TUR-Bt
11	Male	80	G3	pT3	Total Cystectomy
12	Male	73	G2 > G3	pT1	TUR-Bt

WHO, World Health Organization; TUR-Bt, transurethral resection of the bladder tumor